PAPER

Photosensitized electron transfer within a self-assembled *nor*harmane–2′-deoxyadenosine 5′-monophosphate (dAMP) complex†

M. Micaela Gonzalez,[a] Federico A. O. Rasse-Suriani,[b] Carlos A. Franca,[c] Reinaldo Pis Diez,[c] Yousef Gholipour,[d] Hiroshi Nonami,[d] Rosa Erra-Balsells*[a] and Franco M. Cabrerizo*[b]

*Nor*harmane is a compound that belongs to a family of alkaloids called β-carbolines (βCs). These alkaloids are present in a wide range of biological systems, playing a variety of significant photo-dependent roles. Upon UV-A irradiation, βCs are able to act as efficient photosensitizers. In this work, we have investigated the photosensitized oxidation of 2′-deoxyadenosine 5′-monophosphate (dAMP) by *nor*harmane in an aqueous phase, upon UV-A (350 nm) irradiation. The effect of the pH was evaluated on both the interactions between *nor*harmane and dAMP in the ground and electronic excited states, and on the dAMP photosensitized oxidation. A quite strong static interaction between *nor*harmane and dAMP was observed, especially under those pH conditions where the protonated form of the alkaloid is present (pH < 7). Theoretical studies were performed to further characterize the static complex structure. The participation of reactive oxygen species (ROS) in the photosensitized reaction was also investigated and the photoproducts were characterized by means of UV-LDI-MS and ESI-MS. All the data provided herein indicate that electron transfer (Type I) within a self-assembled *nor*harmane–dAMP complex is the operative mechanism in the dAMP photosensitization.

Introduction

β-Carboline (βC) alkaloids are present in a great variety of living systems.[1–7] *In vivo* they may easily be formed by cyclization of indoleamines with aldehydes.[8] In a mammalian body, these alkaloids occur as normal constituents in eyes, skin, plasma, platelets and urine.[7,9,10] However, under certain conditions such as after alcohol intake and smoking βCs' basal levels (~ 0.1 nmol l^{-1})[7,10] are considerably increased (*i.e.*, ~ 1 nmol l^{-1}).[7,11]

The participation of several βCs in different photosensitizing processes has been demonstrated. Upon UV-A irradiation βCs are able to induce damage in mammalian cell chromosomes,[12,13]

to inactivate bacteria[14,15] and viruses.[16] In plants, the biological role of some βCs could be related with the defense response by means of phototoxic effects against insects, webworms, *etc.*[17] However, the main photobiological role of these alkaloids and the molecular mechanisms involved in those photosensitized processes are, up to now, still poorly understood.

During the last few years the photophysics and the photo-chemistry of βCs in an aqueous phase have been well investigated.[18–20] Although this, only a few studies regarding the photosensitizing properties of these alkaloids have been described.[21,22] Recently, we have demonstrated that, upon UV-A irradiation, βCs derived from 9*H*-pyrido[3,4-*b*]indole or *nor*harmane (Scheme 1) are able to induce DNA photodamage.[23,24] It has been shown that the interaction of βCs with DNA as well as the DNA photodamage strongly depend on the pH of the solution. Mechanistic aspects have been also analyzed reaching the conclusion that electron transfer processes (Type I mechanism) are involved in both, the induction of DNA single-strand breaks (SSB) and in the photosensitized generation of Fpg-sensitive DNA modifications (Fpg or formamidopyrimidine-DNA glyco-sylase recognizes 8-oxoGua, formamidopyrimidines, 2,2,4-tri-aminooxazolone and AP sites). Besides, photoexcited harmine was the only investigated βC that showed to induce the formation of cyclobutane pyrimidine dimers *via* triplet–triplet energy transfer.

However, several points still need to be addressed. No information is available regarding the nature of the interaction between βCs, in their electronic excited states, and the DNA
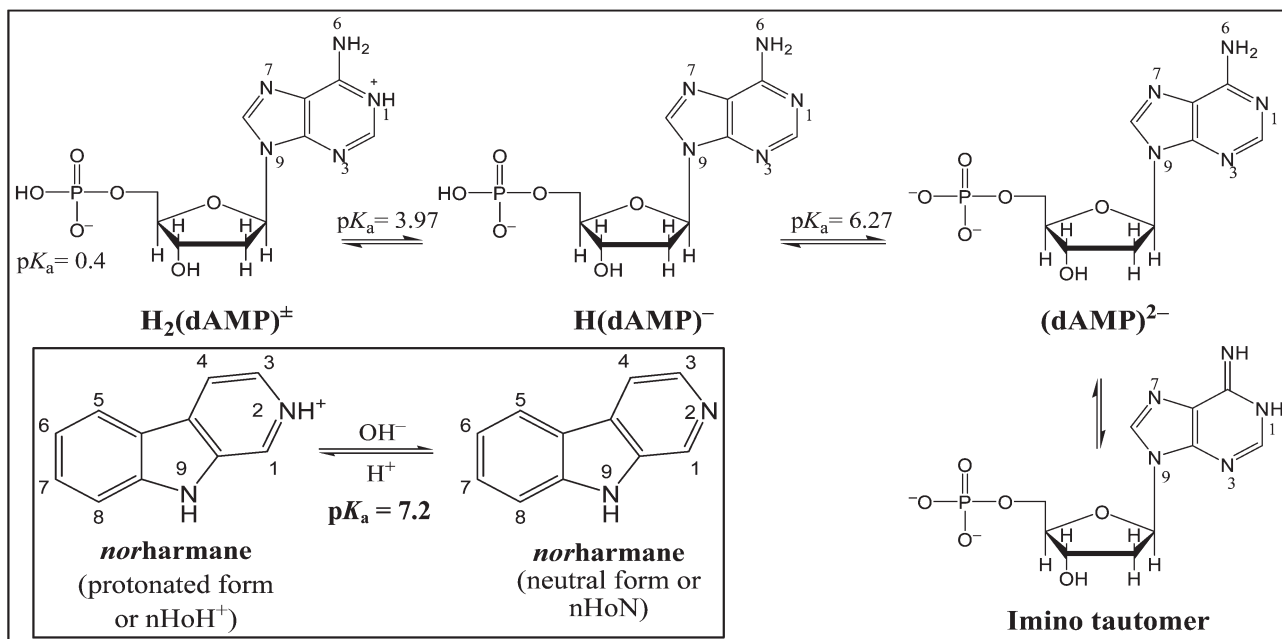
[a]*CIHIDECAR – CONICET, Departamento de Química Orgánica, Facultad de Ciencias Exactas y Naturales, Universidad de Buenos Aires, Pabellón 2, 3p, Ciudad Universitaria, (1428) Buenos Aires, Argentina. E-mail: erra@qo.fcen.uba.ar*
[b]*Instituto de Investigaciones Biotecnológicas – Instituto Tecnológico de Chascomús (IIB-INTECH), Universidad Nacional de San Martín (UNSAM) – Consejo Nacional de Investigaciones Científicas y Técnicas (CONICET), Intendente Marino Km 8.2, CC 164 (7130) Chascomús, Argentina. E-mail: fcabrerizo@intech.gov.ar*
[c]*CEQUINOR – CONICET, Facultad de Ciencias Exactas, Universidad Nacional de la Plata, calle 47 y 115, (1900) La Plata, Argentina*
[d]*Plant Biophysics/Biochemistry Research Laboratory, College of Agriculture, Ehime University, 3-5-7 Tarumi, (790-8566) Matsuyama, Japan*
†Electronic supplementary information (ESI) available. See DOI: 10.1039/c2ob26462e

This journal is © The Royal Society of Chemistry 2012

Org. Biomol. Chem., 2012, **10**, 9359–9372 | 9359

Scheme 1 Molecular structure of *nor*harmane and 2′-deoxyadenosine 5′-monophosphate (dAMP) and the corresponding acid–base equilibrium observed in the aqueous phase in the pH range of 2–11.

monomers (nucleotides). The question is: do βCs react specifically with a given nucleotide and/or with a specific DNA-base sequence? In this context, a research program related with the study of the photosensitizing properties of βCs on 2′-deoxyribonucleotides and oligonucleotides (polydG, polydA, *etc.*) is in progress in our laboratory.

Here we describe the first *in vitro* study of the photosensitized (UV-A) oxidation of 2′-deoxyadenosine 5′-monophosphate (dAMP) by *nor*harmane (Scheme 1) in an aqueous solution.[25] Particularly, the pH-dependence on both the molecule interactions in the ground and electronic excited states and on the photosensitizing properties was investigated.

Experimental methods

General

*Nor*harmane (>98%) from Sigma-Aldrich was used without further purification. 2′-Deoxyadenosine 5′-monophosphate (dAMP) and other chemicals were used as received (Sigma-Aldrich). The pH of the aqueous solutions was adjusted by adding drops of HCl or NaOH solutions from a micropipette. For experiments in which oxygen was removed by bubbling with Ar or N_2, the pH was adjusted after an initial period of bubbling to account for any changes in pH associated with CO_2 loss. The concentrations of the acid and the base used for this purpose ranged from 0.1 M to 2 M. In experiments using D_2O as a solvent, D_2O (>99.9%; Euriso-top or Aldrich), DCl (99.5%; Aldrich) in D_2O, and NaOD (Aldrich) in D_2O were employed.

Binding studies

UV-vis spectrophotometric analysis. The interaction of *nor*harmane with dAMP was studied by UV-vis absorption

spectroscopy using the Benesi–Hildebrand equation. The spectra were recorded on a Perkin Elmer lambda 25 spectrophotometer. Measurements were made in quartz cells of 1 cm optical-path length, at room temperature. The concentrations of *nor*harmane aqueous solutions were 262, 20 and 149 µM at pH 2.5, 5.4 and 10.5, respectively. Nucleotide concentration varied from 0 to 50 mM in the experiments performed at pH 5.4 and 10.5. In measurements carried out at pH 2.5 the maximum dAMP concentration reached was 11 mM, due to its low solubility under this pH condition. Experimental difference (ED) spectra were obtained by subtracting the spectrum at 0 µM of dAMP from the subsequent spectra recorded at different dAMP concentrations.

Assuming a 1 : 1 stoichiometry for complexes, the association constants (K_G) can be estimated by using the Benesi–Hildebrand equation (eqn (1))

$$\frac{1}{\Delta A} = \frac{1}{(\varepsilon_{nHo\cdot B} - \varepsilon_{nHo})\,[nHo]_o} \frac{1}{[nHo]_o} + \frac{1}{K_G(\varepsilon_{nHo\cdot B} - \varepsilon_{nHo})\,[nHo]_o} \frac{1}{[B]}$$

(1)

where $\varepsilon_{nHo\cdot B}$ and ε_{nHo} are the molar absorption coefficients of the *nor*harmane·dAMP complex (nHo·B) and nHo, respectively, at the titration wavelength. ΔA is the change of absorbance, at dAMP concentration ([B]), relative to the completely free *nor*harmane ([nHo] = 0 M) at this wavelength.

Fluorescence measurements. Fluorescence measurements were performed using a single-photon-counting equipment FL3 TCSPC-SP (Horiba Jobin Yvon), on 0.4 × 1 cm path length quartz cells, at room temperature. (i) *Steady-state fluorescence measurements*: corrected fluorescence spectra were recorded. For determining the quenching of fluorescence of *nor*harmane by dAMP, emission spectra of the alkaloid aqueous solution

(20 μM) were recorded in the absence and in the presence of dAMP (from 0 to 15 mM). The experiments were performed under three pH conditions (pH 2.5, 5.4 and 10.5). The fluorescence intensity (I_F) was obtained by integration of the corrected fluorescence spectra over the entire emission profile. (ii) *Time-resolved measurements*: the same set of solutions described above was analyzed by time correlated fluorescence. A NanoLED source (maxima at 341 nm) was used for excitation. The emitted photons, after passing through the iHR320 monochromator, were detected by a TBX-04 detector connected to a TBX-PS power supply and counted by a FluoroHub-B module, controlled using the DataStation measurement control software application. The selected counting time window for the measurement reported in this study was 0–200 ns. Emission decays were monitored at 450 nm. Lifetimes were obtained from the mono-exponential decays observed after deconvolution from the lamp background signal.

Steady-state and time-resolved fluorescence quenching experiments are useful tools that allow us to distinguish between dynamic and static quenching. In the current work, fluorescence quenching data were analyzed as it was previously described.[26,27]

When a dynamic process operates, fluorescence quenching can be evaluated by a Stern–Volmer analysis (eqn (2))

$$I_F{}^0/I_F = \tau_F{}^0/\tau_F = 1 + K_{SV}[Q] = 1 + k_q \tau_F{}^0[Q] \quad (2)$$

where $I_F{}^0$ and I_F are the integrated fluorescence intensities, and $\tau_F{}^0$ and τ_F (s) the fluorescence lifetimes in the absence and in the presence of the quencher, respectively, k_q is the bimolecular quenching rate constant (L mol^{-1} s^{-1}), [Q] is the quencher concentration (mol L^{-1}) and K_{SV} ($= k_q\tau_F{}^0$) is the Stern–Volmer constant (L mol^{-1}). Therefore, if $I_F{}^0/I_F$ *vs.* [Q] and $\tau_F{}^0/\tau_F$ *vs.* [Q] are linear and have the same slope a purely dynamic process can be assumed.

Static quenching also results in a linear relationship between $I_F{}^0/I_F$ and [Q]. In this case, K_{SV} is equal to the equilibrium constant for ground state complex formation. The measurement of τ_F at different quencher concentrations is a reliable method for differentiating between static and dynamic quenching, since in the former case $\tau_F{}^0/\tau_F = 1$.

If both dynamic and static quenching processes are operating, a quadratic plot is observed for $I_F{}^0/I_F$ *vs.* [Q]. This behavior is mathematically expressed by eqn (3)

$$I_F{}^0/I_F = (1 + K_D[Q])(1 + K_{SS}[Q]) \quad (3)$$

where K_D and K_{SS} are the K_{SV} values for the dynamic and static quenching, respectively. K_D is equal to $k_q\tau_F{}^0$ and K_{SS} is the equilibrium constant for complex formation. As τ_F only depends on dynamic quenching, K_D can be obtained from the plot of $\tau_F{}^0/\tau_F$ *vs.* [Q] (eqn (4)).

$$\tau_F{}^0/\tau_F = 1 + K_D[Q] = 1 + k_q\tau_F{}^0[Q] \quad (4)$$

Proton nuclear magnetic resonance (^{1}H-NMR). 500 MHz ^{1}H-NMR spectra were recorded on a Bruker AM-500 spectrometer, using D$_2$O as the solvent.

(i) Self-association constants. Based on previous findings for other quite similar aromatic heterocycles (caffeine, N_6-

dimethyladenosine, *etc.*)[28–31] the indefinite non-cooperative association or isodesmic model (the equilibrium constant for the individual aggregation steps is always the same) for the aggregation process was assumed. An estimation of the self-association constants (K_{sa}), the number of molecules per aggregate (n) and the critical aggregated concentration (c.a.c.) of the associating system can be provided by ^{1}H-NMR data, plotting ln ($-C\,\Delta$) as a function of ln($-C\,\Delta_0$) and fitting by the following curve[30]

$$\ln(-C\,\Delta) = n\ln(-C\,\Delta_0) + \ln(K_{sa}) + \ln(n) - (n-1)\ln(-\Delta_0) \quad (5)$$

where Δ is the observed deviation from the shift of the monomer ($\Delta = \delta_{obs} - \delta_m$) ($\delta_m$ is the chemical shift of the monomer), Δ_0 is the limiting deviation of the aggregate from δ_m ($\Delta_0 = \delta_{aggr} - \delta_m$) and C the global concentration of the species.

Since the fitting is very sensitive to Δ and Δ_0, we extrapolated the values of δ_m and δ_{aggr} (and hence Δ and Δ_0) using a hyperbolic function (see below) mimicking the plot of the chemical shift δ_{obs} as a function of the reciprocal concentration ($1/C$). Such a plot provides the critical concentrations for aggregation (c.a.c.) which is found at the intersection of the two tangents to the curve.[32] As the hyperbolic curve would never cross the vertical axis at null concentrations, we allowed the curve to shift along the horizontal axis by a quantity b using the following equation:

$$\delta_{obs} = \delta_m + B/(1/C + b) \quad (6)$$

where B is a parameter to shift the curve along the vertical axis. Regression analysis gave the values of δ_m and δ_{aggr} (δ_{obs} for $1/C = 0$) and, consequently, Δ and Δ_0 to be used in eqn (5).

(ii) Binding constants (K_G) between nor*harmane and dAMP.* ^{1}H-NMR spectra of a *nor*harmane D$_2$O solution were recorded in the absence and in the presence of increasing amounts of dAMP. K_G values were calculated by standard regression analysis using eqn (7) to fit experimental data

$$\Delta = \Delta_o C_M{}^{free}/(1/K_G + C_M{}^{free}) \quad (7)$$

where Δ is the change of the chemical shift of nHo ($= \delta_{obs}{}^{nHo} - \delta_m{}^{nHo}$), Δ_o is its limiting value when it is fully complexed and $C_M{}^{free}$ is the experimental dAMP concentration corrected by[33,34]

$$C_M{}^{free} = C_M - C_L\,\Delta/\Delta_o \quad (8)$$

where $C_M{}^{free}$ is the free dAMP concentration, and C_M and C_L are the total concentration of dAMP and *nor*harmane, respectively.

Computational methods

A very large number of conformers both for protonated and neutral forms of *nor*harmane and for the (dAMP)$^{2-}$, H(dAMP)$^-$ and H$_2$(dAMP)$^\pm$ species were explored. The complexes that could be formed by those compounds at different pH were also evaluated. Starting geometries for conformational searching of complexes were constructed to take the pH-system into account. For pH 2.5 and pH 5.4, complexes were built from protonated *nor*harmane and H$_2$(dAMP)$^\pm$ and H(dAMP)$^-$, respectively. On the other hand, for pH 10.5, the complex was formed by neutral *nor*harmane and (dAMP)$^{2-}$.

We applied genetic algorithms as implemented in the Balloon program[35] to obtain a set of starting geometries. These geometries were further optimized using the PM6-DH+ method available in the MOPAC software package.[36] Optimizations were done taking into account solvent effects (water) through a polarizable continuum method. For each system under study those conformations within 2 kcal mol^{-1} from the most stable conformer were considered for averaging the heat of formation according to a Maxwell–Boltzmann distribution at 298 K.

Instrumentation and approaches for dAMP photosensitization experiments

Elapsed irradiation. Aqueous βC solutions were irradiated at 350 nm in 1 cm quartz cells at room temperature with a Rayonet RPR lamp (bandwidth ∼20 nm, Southern N.E. Ultraviolet Co.). Experiments were performed in the presence and absence of air. Oxygen-free solutions were obtained by bubbling with Ar or He for 20 min.

UV-vis analysis. Electronic absorption spectra were recorded on a Perkin-Elmer lambda 25 spectrophotometer. Measurements were made using 1 cm path length quartz cells.

High-performance liquid chromatography (HPLC). A Waters 600E Pump Controller with a UV-vis photo-array detector was used to monitor and quantify the photochemical reactions. Aqueous solutions of commercial standards were employed for the calibration curves. A Supelco-C18 column (250 × 4.6 mm, 5 µm) was used for products separation. The running conditions in gradient elution mode were as follows; the initial eluent was water (pH 7) during 4 min. Then, the eluent was gradually replaced by a mixture of water (pH 3)/methanol (20/80 v/v) and was kept constant for 13 min. After that, the initial eluent (water, pH 7) was used for 15 min before the next sample injection. Flow rate was 1 mL min^{-1}. The injection volume was fixed at 20 µL.

Kinetic analysis of dAMP photosensitization by *nor*harmane. Air-equilibrated aqueous solutions containing *nor*harmane (250–500 µM) and dAMP (250–500 µM) were irradiated at 350 nm. Under these experimental conditions, *nor*harmane was excited, whereas dAMP did not absorb radiation (Fig. 1). In order to avoid interferences between the protonated and the neutral forms of *nor*harmane, experiments were performed in the pH range 5.0–5.5 and 10.2–10.7, where *nor*harmane is present at more than 99% in its protonated (nHoH$^+$) and neutral (nHoN) form, respectively. dAMP instead only shows the acid–base equilibrium where the phosphate group is involved (Scheme 2). It is noteworthy that, in the whole concentration range investigated, less than the 3% of *nor*harmane and dAMP are complexed. The photochemical reactions were followed by UV-visible spectrophotometry and HPLC.

Thermal reactions between *nor*harmane and dAMP were discarded after control experiments performed by keeping solutions containing both compounds in the dark. These experiments were carried out under different conditions (concentration, pH and time). In another set of control experiments, dAMP solutions were irradiated in the absence of *nor*harmane, and no chemical modification of the nucleotide was detected, discarding, as it was expectable, direct effects of the radiation on the dAMP molecule.[37,38]

pH or pD	Complex	Abbreviation	dAMP structure
2.5	nHoH$^+$ / H$_2$(dAMP)$^\pm$	S2.5	
5.4	nHoH$^+$ / H(dAMP)$^-$	S5.4	
10.5	nHoN / (dAMP)$^{2-}$	S10.5	

Scheme 2 *Nor*harmane and 2′-deoxyadenosine 5′-monophosphate (dAMP) complex present under the three different pH conditions investigated in this work.
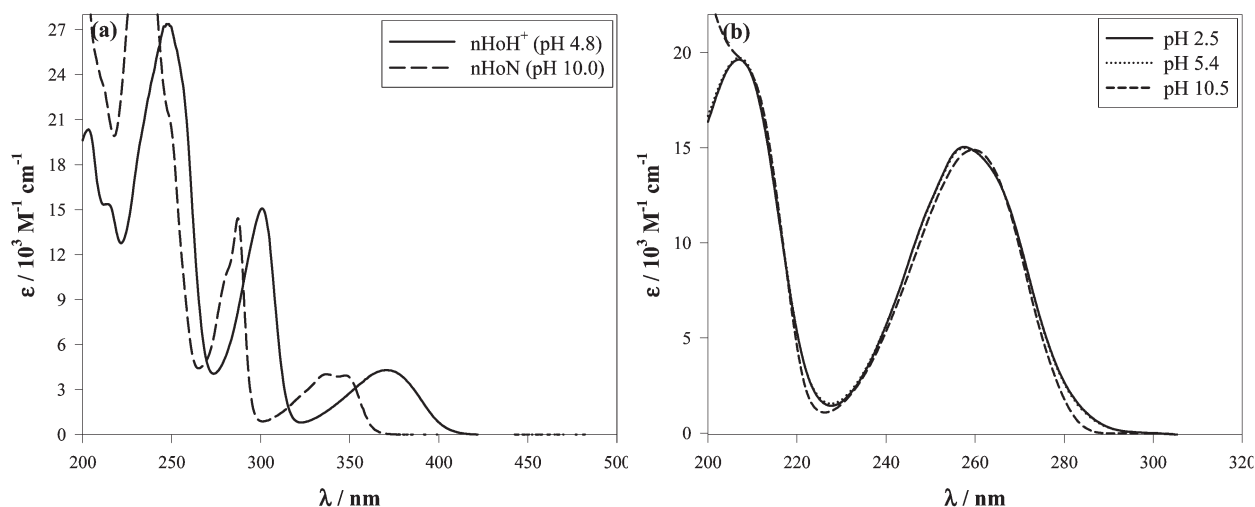
Fig. 1 (a) UV-vis absorption spectra of the protonated and neutral forms of *nor*harmane (nHoH$^+$ and nHoN, respectively) recorded in air-equilibrated aqueous solutions. (b) UV-vis absorption spectra of dAMP in an aqueous solution under the whole pH range investigated in the present work.

O₂ concentration measurements. The O₂ consumption during irradiation was measured with an O₂-selective electrode (Orion 37-08-99; control module: Consort C832 multichannel analyser). The solutions and the electrode were placed in a closed glass-cell of 130 mL.

Detection and quantification of H₂O₂. For the determination of H₂O₂, a Cholesterol Kit (Wiener Laboratorios S.A.I.C.) was used. H₂O₂ was quantified after the reaction with 4-aminophenazone and phenol, following the methodology described elsewhere.[39]

Mass spectrometry analysis. Irradiated and non-irradiated mixture solutions of *nor*harmane and dAMP were analyzed by electrospray ionization mass spectrometry (ESI-MS) and UV-laser desorption ionization time-of-flight mass spectrometry (UV-LDI-TOF-MS): (a) ESI-MS: measurements were performed with an Applied Biosystems *Mariner* ESI-TOF. 5 to 20 μL of samples were injected into the ionization chamber by a Harvard PHD 2000 infusion pump (5 μL min⁻¹). The mixture MeOH–H₂O (90 : 10 v/v) was used as a stream solvent. The control of the equipment and data acquisition were done by Mariner v. 3.0 software (*Applied Biosystems*). The analysis was carried out in both ion modes and the tip voltage was 5 kV. Irradiated and non-irradiated solutions were diluted 10 times with 50 : 50 (v/v) MeOH–NH₄OAc 10 mM in H₂O before injecting into the equipment. Standard stock solutions were used for calibration. (b) UV-LDI-TOF-MS: measurements were performed with an Applied Biosystems Voyager DE-STR laser desorption-TOF-MS. The spectrometer was equipped with a pulsed nitrogen laser (λ_{em} 337 nm; pulsed with 3 ns) tunable PDE and PSD mode as described elsewhere.[40] The samples were irradiated just above the threshold laser power for obtaining molecular ions. Usually 100 spectra were accumulated. All the samples were measured in the linear modes, in both positive- and negative-ion modes. Irradiated and non-irradiated solutions were deposited directly onto the probe without adding a matrix. Typically 1 μL of the solution was placed on the sample probe tip and the solvent was removed by blowing air at room temperature. For calibration, matrix and calibrant stock solutions as well as the calibrant–matrix deposits on the probe were prepared as described elsewhere.[40]

Results and discussion

In aqueous media, in the pH range 2–12, *nor*harmane and dAMP show several acid–base equilibria (Scheme 1). *Nor*harmane shows a very distinctive UV-vis absorption spectrum depending on the pH solution (Fig. 1) because different molecular species are formed. These changes in the electronic ground state distribution have a strong effect on its photochemical and photophysical properties.[18–20] In this regard, we decided to examine the dependence of the *nor*harmane–dAMP interaction and the *nor*harmane capability to photooxidize dAMP on the pH.

Molecular interaction between *nor*harmane and dAMP. Spectroscopic studies

Although the interaction between several βC derivatives and nucleotides has been described,[21,41,42] it is noteworthy that these studies have been performed in solvents and pH conditions rather different from those used in the present work. We examined first the pH-dependence of the *nor*harmane–dAMP interaction by UV-vis absorption, ¹H-NMR and fluorescence spectroscopy.

In order to simplify the analysis, the binding strength of the *nor*harmane–dAMP complex was analyzed under three different pH conditions (2.5, 5.4 and 10.5). At each pH only one acid–base form of each analyte is present in the mixture solution (Scheme 2).

UV-vis absorption spectroscopy. UV-vis spectra of *nor*harmane were recorded in the presence of increasing amounts of dAMP. Fig. 2 shows, as a representative example, results obtained at pH 5.4. Spectra recorded under other pH conditions are shown as ESI.† Despite the minor changes shown in some cases, a clear pH-dependence is observed. This fact indicates that both acidic and basic forms of *nor*harmane (in their electronic ground states) interact with dAMP. In all the cases, the small changes observed in the absorption spectra were accompanied by the appearance of, at least, two isosbestic points (see λ_{iso} in Table 1).

The corresponding association constants (K_G) were estimated by using the Benesi–Hildebrand equation (eqn (1)). Representative plots of the experimental data obtained at pH 5.4 are shown as an inset in Fig. 2. In every instance, experimental data showed a linear behavior when fitted according to eqn (1). The value of K_G obtained from the slope and intercept of these plots listed in Table 1 shows a clear correlation between the chemical nature of the molecules present at a given pH and the strength of the interaction that can be explained in terms of electrostatic interaction (see discussion below). The trend observed was: $K_G^{(pH\ 5.4)} > K_G^{(pH\ 10.5)} > K_G^{(pH\ 2.5)}$.

¹H-NMR analysis. Results shown above were further supported by ¹H-NMR analysis. The interaction between *nor*harmane and dAMP was characterized by monitoring the chemical shift deviations of *nor*harmane proton signals upon
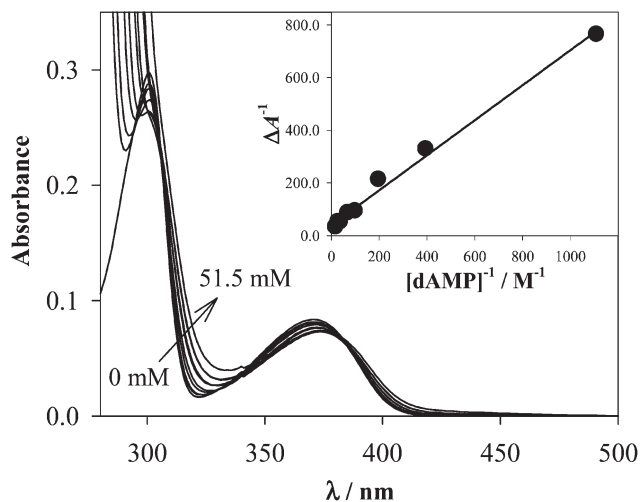
Fig. 2 UV-vis absorption spectra of *nor*harmane (20 μM, pH 5.4) in the presence of increasing amounts of dAMP (see arrows). Inset: a representative Benesi–Hildebrand plot.

This journal is © The Royal Society of Chemistry 2012

Org. Biomol. Chem., 2012, **10**, 9359–9372 | 9363

addition of increasing amounts of dAMP to a D$_2$O solution of *nor*harmane.

(i) Determination of nor*harmane and dAMP self-association constants (K_{sa}^{nHo} and K_{sa}^{dAMP}).* To begin with, since aromatic molecules tend to aggregate in aqueous solutions, the self-association tendency of *nor*harmane and dAMP was separately evaluated. These analyses provide the optimal concentration values to be used in the experiments to study the interaction between *nor*harmane and dAMP without the interference of homo-multimeric *nor*harmane and/or dAMP forms.

The changes in the chemical shift of the analyte proton signals as a function of its concentration were determined at three pH values. Fig. 3a (inset) shows a representative example of the chemical shift of the C1–H proton of nHoH$^+$. By fitting these results with eqn (5) it was possible to obtain the self-association strength described by an equilibrium constant (K_{sa}^{nHoH+},

in M^{-1}) as well as the number of molecules per aggregate (n) present under each pH condition. In the particular case shown in Fig. 3a, the value of n was ∼2, suggesting that, in the concentration range used, the predominant aggregated species formed was a dimer of nHoH$^+$, with a K_{sa}^{nHoH+} value of 6 ± 1 M^{-1}. In order to determine the values of the critical concentration for aggregation (c.a.c.), experimental data were plotted and analyzed according to eqn (6) (Fig. 3b) yielding a c.a.c. value of 4 ± 1 mM. Similar behaviors were observed under all the pH conditions investigated where K_{sa}, c.a.c. and n were estimated (Table 2).

From Table 2 several points should be highlighted:

• Self-association constant (K_{sa}) values obtained for *nor*harmane in aqueous media are in good agreement with those reported elsewhere for other heterocyclic aromatic compounds.

• The K_{sa} value obtained for the neutral *nor*harmane (K_{sa}^{nHoN}) is higher than that observed for its protonated form (K_{sa}^{nHoH+}). Certainly, intermolecular electrostatic repulsions due to the

Table 1 Binding constants (K_G and $K_{G'}$) between *nor*harmane and dAMP and Stern–Volmer constants for static and dynamic quenching of the fluorescence of *nor*harmane by dAMP (K_{SS} and K_D, respectively)

		pH or pD 2.5 S2.5	pH or pD 5.4 S5.4	pH or pD 10.5 S10.5
UV-vis	K_G/M^{-1} ^{a}	22 ± 6	64 ± 8	39 ± 8
	λ_{iso}/nm^b	328 and 388	328 and 383	307 and 353
^{1}H-NMR	$K_{G'}$/M^{-1} ^{c}	13 ± 3	75 ± 9	26 ± 5
Emission SS	K_{SS}/M^{-1} ^{d}	17 ± 1	54 ± 7	22 ± 2^f
TR	K_D/M^{-1} ^{d}	0	0	139 ± 3
	k_q/10^9 L mol^{-1} s^{-1} ^{e}	—	—	6.7 ± 0.2

^{a} Data obtained from UV-vis spectroscopy analysis. ^{b} λ_{iso} is the wavelength of the isosbestic points in UV-vis spectra (nm). ^{c} Data obtained from ^{1}H-NMR spectroscopy analysis. ^{d} Values obtained from steady-state (SS) and time-resolved (TR) measurements. In SS experiments, samples were irradiated (λ_{exc}) at the corresponding absorption maximum wavelength (Fig. 1), whereas in TR experiments λ_{exc} = 341 nm. ^{e} Bimolecular rate constants for the quenching of the fluorescence of *nor*harmane by dAMP. ^{f} Data obtained from eqn (3), using a K_D value obtained from TR experiments as a fixed value for iteration.

Table 2 Self-association constants (K_{sa}) of *nor*harmane and dAMP evaluated under different pH conditions

Compound	c.a.c.^{a}/mM	n^a	K_{sa} ^{a}/M^{-1}	K_{sa} ^{b}/M^{-1}
H$_2$(dAMP)$^\pm$ (pD 2.5)	6.7 ± 0.7	1.6 ∼ 2	2 ± 1	2.1 ± 0.6^c
H(dAMP)$^-$ (pD 5.4)	11 ± 2	1.9 ∼ 2	2.6 ± 0.9	3.4 ± 0.3^d
(dAMP)$^{-2}$ (pD 10.5)	15 ± 2	1.9 ∼ 2	0.36 ± 0.02	2.1 ± 0.3^e
nHoH$^+$ (pD 5.4)	4 ± 1	1.7 ∼ 2	7 ± 1	—
nHoN (pD 10.5)	nd^f	1.8 ∼ 2	80 ± 16^g	—

^{a} Data represent the average of the values derived from 1H-NMR analysis of different protons (Table SI.1, ESI†). ^{b} K_{sa} values obtained from ref. 43 for 5′-AMP at: ^{c} pD 3.44. ^{d} pD 5.61d and ^{e} pD 8.90. ^{f} nd = not measurable. The c.a.c. value could not be calculated because the experimental data obtained correspond to a very narrow nHoN concentration range (due to its low solubility). Thus, the corresponding δ_{obs} *vs.* [nHoN]$^{-1}$ plot could not be drawn in the wide range needed to obtain a hyperbolic distribution. ^{g} This value might be overestimated due to the extremely low solubility of nHoN in an alkaline aqueous solution. Thus, nHoN concentration could not be increased as much as is needed in order to minimize experimental errors while fitting experimental data with eqn (5).
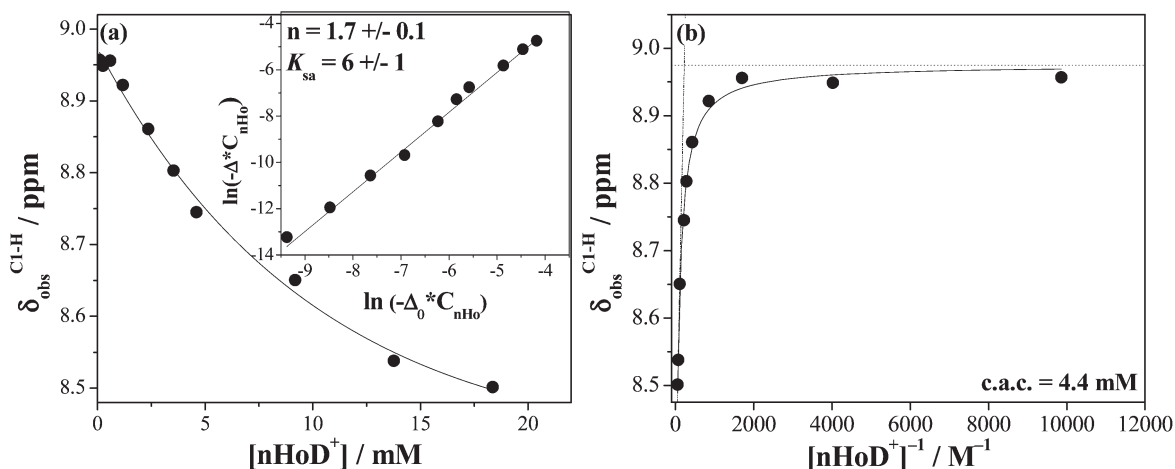
Fig. 3 (a) Chemical shift of C1–H (δ, in ppm) as a function of *nor*harmane concentration, measured in D$_2$O at pD 5.0. Inset: data analysis to obtain the self-association constant (K_{sa}^{nHoH+}) and the number of molecules n per aggregate. (b) Critical aggregation concentration (c.a.c.) calculated from the analysis of the chemical shifts of *nor*harmane C1–H proton observed as a function of [nHoD$^+$]$^{-1}$.

positive net charge localized on the nHoH$^+$ moiety would be the cause of the lower aggregation tendency of nHoH$^+$.

• A clear dependence of K_{sa}^{dAMP} values on the pH was observed. The lowest K_{sa}^{dAMP} value obtained was at pH 10.5 where the predominant species of the nucleotide (dAMP)$^{2-}$ has a -2 net charge on the phosphate group. In this case, the nucleotide molecule can be better solvated by the solvent (water), reducing the chance of self-aggregation. At pH 2.5, H$_2$(dAMP)$^\pm$ is the predominant species in the solution which has a -1 net charge on the phosphate group and a $+1$ net charge on the protonated nucleobase (zwitterionic specie). The experimental value for $K_{sa}^{H_2(dAMP)^\pm}$ is higher than $K_{sa}^{(dAMP)2-}$ in accordance with the lower solubility shown by H$_2$(dAMP)$^\pm$ in water (see below). This is the first time that K_{sa} values of each acid–base form of dAMP are provided, and the values measured substantially agree with those reported in the literature for a related nucleotide, adenosine 5′-monophosphate (AMP).[43]

• dAMP has a lower tendency of self-aggregation (lower K_{sa} value) than *nor*harmane. This fact could be a consequence of repulsion forces due to the negative charge present in the phosphate group of each dAMP moiety. Moreover, this part of the dAMP molecule can be better solvated by water, decreasing the aggregation tendency. On the other hand, the lower solubility of *nor*harmane in H$_2$O is in good agreement with the relative high K_{sa} observed for this alkaloid.

• For both analytes, the n values obtained under all pH conditions were very close to 2, suggesting dimeric aggregation.

• It is generally accepted that self-association of these species occurs *via* aromatic-ring stacking of the molecules, which proceeds beyond the dimer stage. The upfield ^{1}H-NMR shifts of the resonances observed for both the *nor*harmane and the nucleobase protons while increasing their concentration confirm that the association occurs *via* stacking of the aromatic moieties (hydrophobic–hydrophobic interaction).

(ii) Determination of norharmane–dAMP binding constants (K$_G$). In order to evaluate the equilibrium constant, the initial concentration of each molecule was kept below the c.a.c. previously determined. Under these conditions, both analytes were in their monomeric forms.[44] A solution of *nor*harmane (ranged from 0.5–1.0 mM) was titrated with a concentrated solution of dAMP and the corresponding ^{1}H-NMR spectra were recorded under three different pH conditions (pH 2.5, 5.4 and 10.5). Fig. 4 shows a representative example of the chemical shift of the C1–H proton of *nor*harmane (see Scheme 1) observed at the three pH values investigated. The upfield ^{1}H-NMR chemical shifts observed for the proton signal as a function of dAMP concentration suggest that the association between these two molecules occurs, at least partially, *via* stacking (see discussion in theoretical analysis below).

Fitting the experimental data by using eqn (7) and (8), $K_{G'}$ values of (13 ± 3) M^{-1}, (75 ± 9) M^{-1} and (26 ± 5) M^{-1} were calculated at pH 2.5, 5.4 and 10.5, respectively (Table 1). These data substantially agree with those obtained from UV-vis titration experiments (see above). In brief, the trend for $K_{G'}$ values observed as a function of the pH was: $K_{G'}^{(pH\ 5.4)} > K_{G'}^{(pH\ 10.5)} > K_{G'}^{(pH\ 2.5)}$ (see discussion below).

Fluorescence emission spectroscopy. Corrected emission spectra of *nor*harmane were recorded in the presence and in the
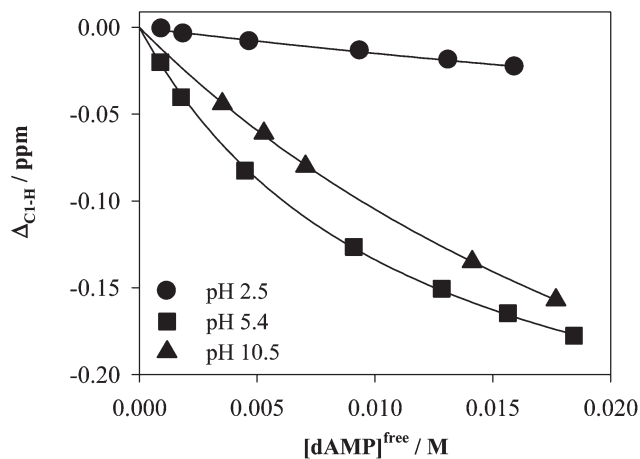
Fig. 4 Chemical shift ($\Delta = \delta_{obs}^{nHo} - \delta_{m}^{nHo}$) of the *nor*harmane C1–H signal as a function of the free dAMP concentration.
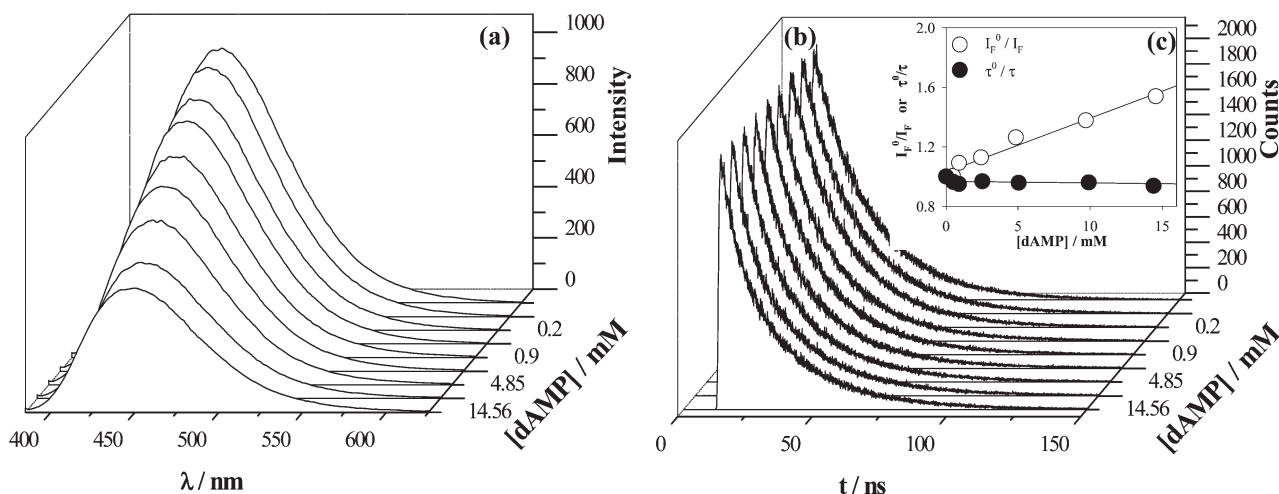
absence of dAMP. Experiments were carried out in *nor*harmane aqueous solutions ($\sim$20 μM) containing different concentrations of the nucleotide under three different pH conditions: 2.5, 5.4 and 10.5. In all cases, a decrease in the fluorescence intensity was observed and the wavelength of the emission maximum remained unchanged. In addition, in time-resolved experiments first-order kinetics were observed for all fluorescence decays of *nor*harmane in the presence of different dAMP concentrations. Fig. 5 shows, as a representative example, results obtained at pH 5.4.

(i) Analysis under acidic conditions (pH 2.5 and 5.4). In steady-state experiments, I_F^0/I_F as a function of the nucleotide concentration was linear. However, time-resolved experiments did not show any dependence of the fluorescence lifetimes (τ_F) on the dAMP concentration. The corresponding τ_F remained unchanged ($\sim$21 ns), under our experimental conditions. Fig. 5c shows the results obtained at pH 5.4. Results obtained under other pH conditions are detailed in ESI (Fig. SI.6a†).

These two facts are in accordance with a purely static quenching dominating process. Comparison of K_{SS} values calculated from fluorescence steady-state, UV-vis and ^{1}H-NMR studies reveals that there are no significant differences between the values obtained from these three groups of experimental data (Table 1). Thus, nHoH$^+$ forms a static complex in its electronic ground state with both H$_2$(dAMP)$^\pm$ and H(dAMP)$^-$.

(ii) Analysis under alkaline conditions (pH 10.5). Steady-state experiments performed in alkaline media showed an increased efficiency of fluorescence quenching by the nucleotides in comparison with that observed in acidic media (nHoH$^+$). In this case, the variation I_F^0/I_F as a function of the nucleotide concentration followed a non-linear Stern–Volmer behavior (Fig. SI.6b, ESI†). The curve could be fitted with eqn (3), suggesting that the quenching observed is a combination of dynamic and static processes (see the Experimental section).

Under these pH conditions, time resolved experiments were also carried out. Contrary to what was previously described in the literature,[45] the τ_F^0 value (the fluorescence lifetime of the singlet excited state of *nor*harmane in the absence of dAMP) obtained herein was $\sim$21 ns. This value is in good agreement with the fact

This journal is © The Royal Society of Chemistry 2012

Org. Biomol. Chem., 2012, **10**, 9359–9372 | 9365

Fig. 5 (a) Corrected fluorescence emission spectra of a *nor*harmane aqueous solution (20 μM, pH 5.4, λ_{exc} = 370 nm) in the presence of different dAMP concentrations. (b) Fluorescence decays of *nor*harmane emission as a function of dAMP concentration (λ_{exc} = 341 nm, λ_{em} = 450 nm). (c) Inset: Stern–Volmer plots of the fluorescence intensities (I_F) and the fluorescence lifetimes (τ_F).

that, even at pH 10.5, the emitting species is $[nHoH^+]^*$.[46] A strong decrease of τ_F was observed when dAMP concentration was increased and the corresponding Stern–Volmer plot showed a linear dependence of τ_F^0/τ_F *vs.* [dAMP] (Fig. SI.6b, ESI†). The corresponding K_D and K_{SS} values, listed in Table 1, reveal that the quenching of the nHoN fluorescence by $dAMP^{2-}$ is mainly dynamic and only a very small contribution of static quenching occurs in the dAMP concentration range analyzed.

In alkaline experiments a value of $(6.7 \pm 0.2) \times 10^9$ L mol^{-1} s^{-1} for the bimolecular quenching rate constant (k_q), calculated from K_D values ($k_q = K_D/\tau_F^0$), was obtained. This value is under the diffusion-controlled limits and it is quite similar to k_q values reported in the literature for related compounds (*i.e.*, fluorescence quenching of pterins by dAMP).[27]

Comparison between K_G, $K_{G'}$ and K_{SS} values

From experiments described above several points rise to the surface:

• A strong pH effect for the association process between *nor*harmane and dAMP was observed ($K^{(pH\ 5.4)} > K^{(pH\ 10.5)} > K^{(pH\ 2.5)}$). The different behavior of acidic and basic forms of *nor*harmane towards quenching by dAMP may be due to the difference in the charge of the molecules.

The highest binding constant values were observed at pH 5.4 where a positive net charge in the *nor*harmane moiety (nHoH$^+$) and a negative charge in the phosphate group of the nucleotide moiety H(dAMP)$^-$ would promote the interaction.

On the other hand, K values obtained in an alkaline solution (pH 10.5) were slightly lower than that obtained at pH 5.4. This fact can be the consequence of the lack of the positive charge in the *nor*harmane moiety (nHoN) that diminishes the coulombic attraction.

Finally, the lower K values were observed at pH 2.5. At this pH, although a negative charge is localized in the phosphate group that can interact with nHoH$^+$ by coulombic attraction, a simultaneous non-negligible contribution of the electrostatic

repulsion between nHoH$^+$ and the positive net charge localized in the adenine base H$_2$(dAMP)$^{\pm}$ would diminish the molecule interaction necessary for the quenching process. Therefore this charge repulsion, which does not take place under the other two pH conditions investigated, may inhibit the formation of the complex between nHoH$^+$ and the nucleobase.

• A total quenching process is much more efficient in alkaline than in acidic media due to the high contribution of the dynamic quenching processes in addition to a small static complexation. Taking into account that upon UV irradiation the excited state of the protonated form ($[nHoH^+]^*$) is the predominant species, even at pH 10.5, then $[nHoH^+]^*$ would be involved in the dynamic deactivation processes observed.

However, the fact that the binding constant obtained from steady-state experiments (K_{SS}) is similar, within the experimental error, to those obtained from the UV-vis and ^{1}H-NMR spectroscopy reveals that in an alkaline solution the neutral form of *nor*harmane in its electronic ground state is involved in the static complexation (no exciplex between $[nHoH^+]^*$ and dAMP is formed).

Theoretical analysis of the molecule interactions

Noncovalent interactions are of fundamental importance for exploring molecular systems in biological disciplines. Theoretical description of these interactions is difficult, mainly because they are much weaker than covalent interactions and also the key role played by the London dispersion energy must be taken into account. Pavel Hobza *et al.* introduced an extension of the semi-empirical PM6 method in two directions. The first one includes an empirical correction to the dispersion energy that improves the description of complexes controlled by the dispersion energy. The second one introduces an additional electrostatic term that improves the description of hydrogen-bonded complexes. The resulting method, PM6 with corrections for dispersion and hydrogen bonding, was labeled PM6-DH.[47]

The PM6-DH technique was further tested for various extended stacked complexes (*i.e.*, porphine dimer, graphene models with DNA bases, and base pairs). It was shown that the method provides stabilization energies that agree very closely with the benchmark values obtained by much more expensive methods such as DFT-D, SCS-MP2 and MP2.5.[47] Furthermore, it was also shown that PM6-DH can be used for geometry optimizations of rather large biomolecules, such as a DNA tetramer for example.[47]

In the present work the dispersion- and hydrogen bonding-corrected PM6 method was used to explore the complexes that could originate from the combination of neutral and protonated forms of *nor*harmane and the $(dAMP)^{2-}$, $H(dAMP)^-$ and $H_2(dAMP)^\pm$ species, with special emphasis on the interaction energy.

In first place, a conformational search for the three forms of the free nucleotide was done. Briefly, $(dAMP)^{2-}$ led to 11 *anti* conformations within the energy penalty of 2 kcal mol^{-1} (including the most stable) and only to one *syn* conformation. In the case of $H(dAMP)^-$, just one *syn* conformation and 9 *anti* conformations (including the most stable one) were found, within the energy penalty. The lowest energy conformation for $H_2(dAMP)^\pm$ was found to be a *syn* conformation. Other 5 *syn* conformations and 8 *anti* conformations were found, within the 2 kcal mol^{-1} range from the most stable species of $H_2(dAMP)^\pm$. The most stable conformation found for every nucleotide form is depicted in Fig. 6.

It is important to note that both in the solid state and in solution, nucleosides and nucleotides exist predominantly in the so-called *anti* conformation. This means, in the case of purines, that the N9–C8 bond projects onto or near the sugar ring. In the *syn* conformation, on the other hand, the N9–C4 bond projects onto or near the sugar ring (see Scheme 1).[48] A possible explanation of the existence of the lowest energy *syn* conformation in $H_2(dAMP)^\pm$ could be that the positive charge localized in the adenine moiety is closer to the phosphate negative group when the N9–C4 bond projects onto the sugar ring, thus giving place to an attractive electrostatic interaction.

In the case of *nor*harmane–dAMP complexes, the searching with the genetic algorithms led to 404 conformers for the system at pH 2.5 (S2.5 from now on), 325 conformers for the system at pH 5.4 (S5.4), and 343 conformers for the system at pH 10.5 (S10.5). All those conformers were further optimized at the PM6-DH+ level of theory. As in isolated molecules, those complexes presenting a heat of formation (HOF) up to 2 kcal mol^{-1} above the lowest energy conformer were considered to obtain a statistically averaged HOF for each system. Thus, an approach to the intermolecular interaction energy is given by subtracting the HOFs of nucleotides and *nor*harmane species to the HOF of the complex. In Fig. 7 HOFs together with the lowest energy conformations for S2.5, S5.4 and S10.5 are shown. It can be seen that calculated HOFs are in reasonable agreement with experimental binding constants. The averaged values of binding constants for S2.5, S5.4 and S10.5 displayed in Table 1 suggest that the entropic term $T\Delta S$ must be negative for all the cases, which means that the complexation process leads to highly ordered systems. Besides, a parallel π-stacking interaction is observed in the three systems. Different types of hydrogen bonds can be seen for all conformations too. Complementarily, the lists with the parameters (length, angle) that define the geometry of the hydrogen bonding interaction for each conformation are included in ESI (Tables S1 to S3†).

Photosensitized oxidation of dAMP by *nor*harmane

(i) Kinetic analysis. To find out if *nor*harmane is able to photosensitize dAMP, air-equilibrated aqueous solutions containing *nor*harmane and dAMP were irradiated. Fig. 8 shows, as a representative example, HPLC data analysis obtained at pH 5.4 (system S5.4 = nHoH$^+$/H(dAMP)$^-$). Although the effect was
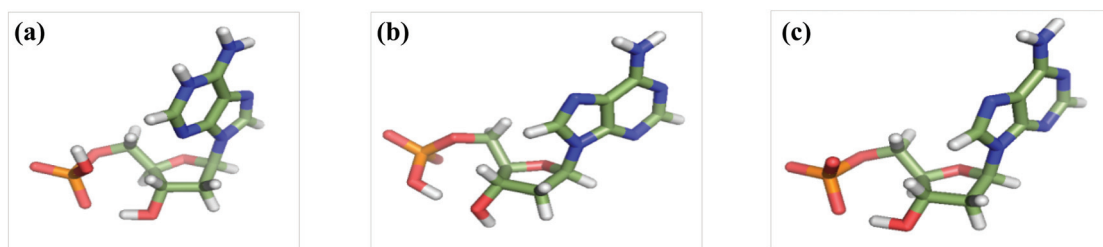

Fig. 6 Most stable nucleotide conformations: (a) $H_2(dAMP)^\pm$, (b) $H(dAMP)^-$ and (c) $(dAMP)^{2-}$.

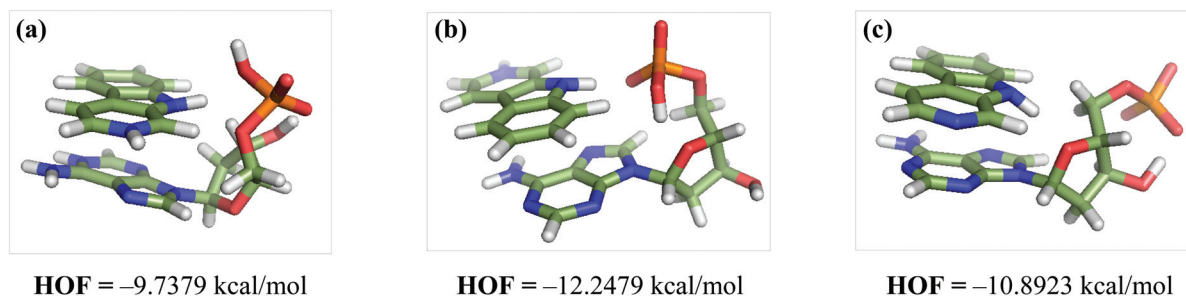**HOF = −9.7379 kcal/mol**   **HOF = −12.2479 kcal/mol**   **HOF = −10.8923 kcal/mol**

Fig. 7 The lowest energy conformation and heat of formation (HOF, in kcal mol^{-1}) for the three complexes: (a) S2.5, (b) S5.4 and (c) S10.5.

This journal is © The Royal Society of Chemistry 2012

Org. Biomol. Chem., 2012, **10**, 9359–9372 | 9367

more pronounced in acidic than in alkaline media, a small decrease of the dAMP concentration as a function of irradiation time was observed, under both pH conditions. The corresponding rate values of dAMP consumption (d[dAMP]/dt), listed in Table 3, show that in the studied process dAMP was chemically modified by UV-A excitation of *nor*harmane. To the best of our knowledge, this is the first time that evidence of photosensitization of dAMP (isolated or included in a nucleic acid molecule) by βC alkaloids is reported.

As was previously described, *nor*harmane has its own photochemical reactions (reactions 1, 10 and 19).[18] Thus, in order to evaluate the fate of these reactions while this alkaloid was irradiated in the presence of dAMP, the change in the *nor*harmane concentration was also monitored and quantified in the irradiated solutions. Fig. 8 shows the results obtained at pH 5.4. With comparative purpose, the kinetics of $nHoH^+$ photochemical reaction in the absence of $H(dAMP)^-$ was also analyzed. The results obtained showed a decrease in the total rate of $nHoH^+$ consumption (d[$nHoH^+$]/dt) from (-0.77 ± 0.03) μM min^{-1} to (-0.66 ± 0.01) μM min^{-1}, in the absence and in the presence of dAMP, respectively. A similar behavior was observed in alkaline media.
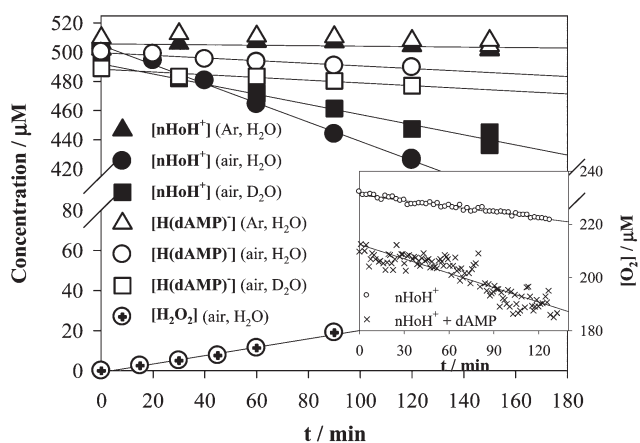
Fig. 8 Evolution of the $H(dAMP)^-$, $nHoH^+$ and H_2O_2 concentrations in air-equilibrated aqueous solutions under UV-A irradiation (350 nm) as a function of irradiation time (pH 5.4, concentrations were determined by HPLC analysis and colorimetric assay). Inset: evolution of the O_2 concentration in an irradiated solution containing $nHoH^+$ (~500 μM) in the absence and in the presence of $H(dAMP)^-$ (~500 μM) at pH 5.4 as a function of irradiation time. Data are shown in a separate plot as the irradiation geometry used was different from that used for the data plotted in the main figure.

At first sight, the d[$nHoH^+$]/dt decrease observed can be explained in terms of $nHoH^+$/$H(dAMP)^-$ interaction. However, under our experimental conditions, less than 3% of the molecules were complexed. Thus, assuming that the very small fraction of complexed $nHoH^+$ follows non-reactive deactivation and also assuming that the change in the solution absorbance due to complexation is negligible, the estimated decrease of d[$nHoH^+$]/dt, due to complex formation, would be lower than 0.02 μM min^{-1}. This value is quite far from the decrease of 0.11 μM min^{-1} observed $(-0.77$ μM min^{-1} $- (-0.66$ μM min$^{-1}) = 0.11$ μM min^{-1}). Therefore, an additional pathway of $nHoH^+$ recovering should be also taken into account.

Based on results already published for related heterocycle compounds[37,38] pathways summarized in reactions 13 to 18 would explain our findings. In these reactions a clear net $H(dAMP)^-$ consumption was observed whereas $nHoH^+$ remained unchanged. The stoichiometric relationship showed in these equations suggests that for each molecule of $nHoH^+$ in its excited state ([$nHoH^+$]*) that reacts with $H(dAMP)^-$, one molecule of the nucleotide is consumed and one molecule of $nHoH^+$ is recovered. Thus, the sum of the $nHoH^+$ and $H(dAMP)^-$ consumption rates observed (d[$nHoH^+$]/dt = 0.66 μM min^{-1} and d[$H(dAMP)^-$]/dt = 0.09 μM min^{-1}) and the estimated decrease of d[$nHoH^+$]/dt due to complexation (0.02 μM min^{-1}) yield a total value of 0.77 μM min^{-1}. This value agrees with the experimental d[$nHoH^+$]/dt observed in the absence of $H(dAMP)^-$, due to its own photochemistry.

(ii) Role of reactive oxygen species (ROS). Solutions containing *nor*harmane (250–500 μM) and dAMP (250–500 μM), previously purged with Ar, were irradiated. No significant changes were observed neither in the absorption spectra nor in the HPLC analysis of the solutions after more than 150 min of irradiation in the whole pH range investigated (pH from 5.0 to 10.7).

The evolution of the O_2 concentration during the irradiation of air-equilibrated aqueous solutions was monitored using an oxygen electrode in a closed cell. In solutions containing dAMP and *nor*harmane the O_2 concentration decreased as a function of irradiation time. The inset in Fig. 8 shows data acquired under acidic conditions (S5.4). For comparative purpose the [O_2] evolution while a $nHoH^+$ solution (free of $H(dAMP)^-$) was irradiated is also shown. A clear increase in the rate of O_2 consumption was observed when $H(dAMP)^-$ was present in the solution ($-$d[O_2]/dt values were (0.168 ± 0.009) μM min^{-1} and (0.172 ± 0.002) μM min^{-1}, in the absence and in the presence of

Table 3 Rate of consumption of *nor*harmane and dAMP obtained by HPLC analysis

	d[nHo]/dt/μM min^{-1}		d[dAMP]/dt/μM min^{-1}	
Experimental conditions	pH 5 S5.4	pH 10 S10.5	pH 5 S5.4	pH 10 S10.5
nHo (Ar, H_2O)	0	0	—	—
nHo + dAMP (Ar, H_2O)	0	0	0	0
nHo (air, H_2O)	-0.77 ± 0.03	-0.22 ± 0.03	—	—
nHo + dAMP (air, H_2O)	-0.66 ± 0.01	-0.21 ± 0.04	-0.09 ± 0.02	-0.05 ± 0.03
nHo + dAMP (air, D_2O)	-0.35 ± 0.01	-0.37 ± 0.02	-0.06 ± 0.02	-0.05 ± 0.01

H(dAMP)⁻, respectively). These results indicate that the process described in the previous section is the oxidation of H(dAMP)⁻.

The formation of H_2O_2 in air-equilibrated solutions of *nor*harmane and dAMP, upon UV-A (λ_{exc} = 350 nm) excitation, was investigated. H_2O_2 was found to be generated and its concentration increased as a function of irradiation time. Fig. 8 shows results obtained under acidic conditions. The rate of H_2O_2 generated ($d[H_2O_2]/dt$ = (0.20 ± 0.01) μM min⁻¹) was of the same order of magnitude as the rate of H(dAMP)⁻ and/or nHoH⁺ consumption. Results obtained in alkaline solutions followed the same trend suggesting that, under the whole pH range investigated, charge transfer processes were involved. In some way this behavior was expected since in polar and homogeneous media such as water, electron transfer is the operative mechanism in the photooxidation of deoxyadenosine by heterocyclic aromatic compounds.[49]

In order to distinguish if the H_2O_2 detected was formed from the *nor*harmane photochemical reaction (reaction 10) independently of the dAMP photosensitized process, H_2O_2 was also quantified in the *nor*harmane solution irradiated in the absence of dAMP under identical experimental conditions. The $d[H_2O_2]/dt$ obtained under acidic conditions was 0.29 μM min⁻¹. Having in mind that, in the presence of dAMP the own photochemistry of *nor*harmane is decreased in ~15%, it is noteworthy that $d[H_2O_2]/dt$ is decreased in ~30%. The latter value indicates the presence of additional pathways that might contribute to the net H_2O_2 consumption observed (reactions 14, 17 and 18, see below).

Contrary to results described for other nucleotides such as 2′-deoxyguanosine 5′-monophosphate (dGMP),[50] a recent study reported that adenine does not significantly react with $^1O_2$. A value of $(8 \pm 3) \times 10^3$ M⁻¹ s⁻¹ for the rate constant of the chemical reaction (k_r) between $^1O_2$ and dAMP (at pH 5.5) was reported.[37] Certainly, this value is very low, indicating that the chemical reaction between $^1O_2$ and dAMP is negligible. However, bearing in mind that upon UV-A excitation *nor*harmane is able to produce $^1O_2$,[18] the role of this ROS in the photosensitization of dAMP should be investigated.

To begin with, the role of $^1O_2$ in the photosensitized oxidation of dAMP can be evaluated by a simple kinetic analysis. Briefly, taking into account k_r values, the initial dAMP concentration and the $^1O_2$ steady-state concentration ($[^1O_2]_{EE}$), the value of the initial rate of the reaction between $^1O_2$ and dAMP can be calculated (numerical support, ESI†). Clearly, the estimated rates (7 × 10⁻⁴ μM min⁻¹ and 5 × 10⁻⁴ μM min⁻¹ for nHoH⁺ and nHoN, respectively) are negligible in comparison with the experimental rates of dAMP consumption listed in Table 3 ((0.09 ± 0.02) μM min⁻¹ and (0.05 ± 0.03) μM min⁻¹, respectively). Therefore, these results indicate that probably $^1O_2$ is not involved in the mechanism of the dAMP oxidation photoinduced by *nor*harmane.

To confirm this point, comparative photolysis experiments were performed in H_2O and D_2O. Taking into account the longer $^1O_2$ lifetime in D_2O than in H_2O,[51] the photosensitized oxidation of dAMP should be faster in the deuterated solvent if $^1O_2$ would contribute significantly to the reaction. Air-equilibrated solutions containing nHoH⁺ (~500 μM) and H(dAMP)⁻ (~500 μM) in H_2O and D_2O at pH and pD 5.1 and 5.4, respectively, were irradiated under identical conditions. The evolutions of the concentrations of nHoH⁺, H(dAMP)⁻ and H_2O_2 as a function of the irradiation time were analyzed. The results showed that the studied process was not faster in D_2O than in H_2O. The rate of H(dAMP)⁻ disappearance observed in both solvents was similar, within the experimental error ((−0.06 ± 0.02) μM min⁻¹ and (−0.09 ± 0.2) μM min⁻¹ in D_2O and in H_2O, respectively). Experiments performed under alkaline pH conditions showed similar results (Fig. SI.7b, ESI†). These facts suggest that $^1O_2$, albeit present in the reaction mixture, does not participate in the mechanism of dAMP photosensitization. The changes in the rates of *nor*harmane consumption observed in D_2O were discussed elsewhere.[18]

(iii) Mass spectrometry analysis. Electrospray ionization (ESI) mass spectra of irradiated and non-irradiated solutions containing H(dAMP)⁻ and nHoH⁺ (pH 5.0) were registered and compared. Although the analysis was carried out in both positive and negative ion modes (ESI⁺ and ESI⁻), the photoproduct signals were only detected in the former. The signals corresponding to the protonated intact molecular ion of dAMP as [M + H]⁺, where M structures are M_1 = dAMPO₄H₂, M_2 = dAMPO₄NaH and M_3 = dAMPO₄Na₂, were detected at m/z 332.2 ([M_1 + H]⁺ = [dAMPO₄H₃]⁺), 354.1 ([M_2 + H]⁺ = [dAMPO₄NaH₂]⁺) and 376.1 ([M_3 + H]⁺ = [dAMPO₄Na₂H]⁺) (Fig. SI.8, ESI†), together with new signals at m/z 348.5, 369.8 and 392.2 (Fig. SI.9, ESI†) after photosensitization by nHoH⁺.

The new signals were observed in spectra corresponding to both solutions after 4 and 6 h of irradiation and indicate the presence of, at least, one product (arbitrarily named P1). P1 signals observed at m/z 348.5, 369.8 and 392.2 correspond to the protonated intact molecular ion of 8-oxodAMP, a typical product of the photosensitized oxidation of dAMP,[37,52] as [M + H]⁺, with ([M_1 + H]⁺ = [8-oxodAMPO₄H₃]⁺), ([M_2 + H]⁺ = [8-oxodAMPO₄NaH₂]⁺) and ([M_3 + H]⁺ = [8-oxodAMPO₄Na₂H]⁺), respectively.

In order to cross check results obtained from ESI-MS, non-irradiated and irradiated samples were also analyzed by UV-LDI-TOF-MS. Samples were dropped directly onto the sample holder without adding a matrix. *Nor*harmane absorbs the laser radiation, behaving as a MALDI matrix.[53] Results obtained are in good agreement with those got by ESI-MS analysis (Fig. SI.10, ESI†).

Briefly, in positive ion mode, the signals corresponding to the reactants were observed. The signal at m/z 169.0 corresponds to the intact molecular ion of *nor*harmane as [M + H]⁺, while the signals corresponding to the intact molecular ion of dAMP as [M_1 + H]⁺, [M_2 + H]⁺ and [M_3 + H]⁺ were detected at m/z 331.7 ([M_1 + H]⁺ = [dAMPO₄H₃]⁺), 353.6 ([M_2 + H]⁺ = [dAMPO₄NaH₂]⁺) and 375.8 ([M_3 + H]⁺ = [dAMPO₄Na₂H]⁺). In addition, new signals were observed at m/z 369.8 and 391.8 in the spectra corresponding to irradiated solutions. These results indicate the presence of, at least, one product. Although the signal of the intact molecular ion at m/z 348.5 was not observed, in view of ESI-MS results shown above, the named signals may correspond to 8-oxodAMP where peaks at m/z 369.8 and 391.8 are the 8-oxodAMP Na-adducts with structure [M_2 + H]⁺ = [8-oxodAMPO₄NaH₂]⁺ and [M_3 + H]⁺ = [8-oxodAMPO₄Na₂H]⁺, respectively.

It is worth mentioning that UV-LDI mass spectra showed a high number of analyte fragments. Thus, several signals at low

This journal is © The Royal Society of Chemistry 2012
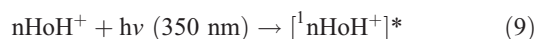
Org. Biomol. Chem., 2012, **10**, 9359–9372 | 9369

m/z values, even in the case of non-irradiated solutions, were observed. Among others minor signals, the simultaneous presence of the fragments at m/z 81.8 ($[PO_3H_3]^+$), 136.1 ($[AH]^+$) and 158.0 ($[ANa]^+$) in the case of non-irradiated nHoH$^+$/dAMP (Fig. SI.11, ESI†), were observed. Together with the signals corresponding to the fragments coming from the reactant, irradiated mixture solutions showed a new signal at m/z 174.0. This fragment corresponds to the loss of the oxidated-base from 8-oxo-7,8-dihydro-2′-deoxyadenosine 5′-monophosphate or 8-oxodAMP (Scheme SI.1, ESI†),[37,54] supporting the hypothesis that 8-oxodAMP is formed during the photooxidation process.

The identification of 8-oxo-7,8-dihydro-2′-deoxyadenosine (8-oxodAMP) as a product of the photosensitized oxidation of dAMP is important, since this compound has been suggested as a product of the photosensitized oxidation of dAMP in DNA through a type I mechanism.[54] Furthermore, the efficient conversion of the radical cation of dAMP (dAMP$^{·+}$) into 8-oxodAMP in aqueous media has been reported.[55] Therefore the results obtained by ESI-MS and UV-LDI-MS analysis together with the already demonstrated capability of *nor*harmane to participate in photoinduced electron transfer reactions support the hypothesis proposed in the previous section that an electron transfer from dAMP to excited *nor*harmane occurs (reaction 13). Then, the radical cation dAMP$^{·+}$ formed may react with O$_2$ to yield 8-oxodAMP.
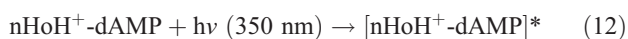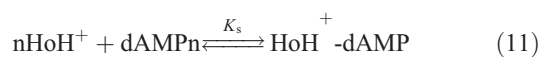
(iv) Mechanism proposed. Taking into account all the results shown in this work, the following mechanism can be proposed for the photosensitized oxidation of dAMP by *nor*harmane:

At pH 5.4. Upon UV-A absorption by the system nHoH$^+$/H (dAMP)$^-$ (S5.4) two groups of photochemical reactions compete for the deactivation of [^{1}nHoH$^+$]*: (iv.1) the intrinsic photochemical reaction of nHoH$^+$ from the free or non-bonded [^{1}nHoH$^+$]* (reactions 9 and 10)[18] and (iv.2) the oxidation of H(dAMP)$^-$ photosensitized by nHoH$^+$ in the heterocomplex (reactions 11–18).

(iv.1) Photochemical reaction of nHoH$^+$.

$$nHoH^+ + h\nu \ (350 \ nm) \rightarrow [^1nHoH^+]^* \qquad (9)$$

$$[^1nHoH^+]^* \rightarrow nHoH^+ \ photoproducts \qquad (10)$$

(iv.2) H(dAMP)$^-$ photooxidation from the heterocomplex. Alternatively, the absorption of the UV-A radiation by nHoH$^+$ present in the heterocomplex previously formed leads to H(dAMP)$^-$ oxidation, through charge transfer processes, yielding [nHoN]$^{·-}$ and dAMP$^{·+}$ radicals. In order to make the reading easier, from now on H(dAMP)$^-$ will be written as dAMP.

$$nHoH^+ + dAMPn \underset{}{\overset{K_s}{\rightleftharpoons}} HoH^+\text{-}dAMP \qquad (11)$$

$$nHoH^+\text{-}dAMP + h\nu \ (350 \ nm) \rightarrow [nHoH^+\text{-}dAMP]^* \qquad (12)$$

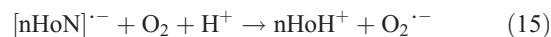$$[nHoH^+\text{-}dAMP]^* \rightarrow [nHoN]^{·-} + dAMP^{·+} + H^+ \qquad (13)$$

Radical ions can recombine (reaction 14), which would be in accordance with the results obtained under anaerobic conditions.

$$[nHoN]^{·-} + dAMP^{·+} + H^+ \rightarrow nHoH^+ + dAMP \qquad (14)$$
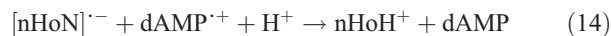
On the other hand, an electron transfer reaction from [nHoN]$^{·-}$ to O$_2$ can take place yielding nHoH$^+$ and O$_2^{·-}$ (reaction 15). The latter radical can react with its conjugated acid (HO$_2^·$) to yield H$_2$O$_2$ (reaction 16) or can react with dAMP$^{·+}$ yielding dAMP (reaction 17) or 8-oxodAMP or other photoproducts (reaction 18).

$$[nHoN]^{·-} + O_2 + H^+ \rightarrow nHoH^+ + O_2^{·-} \qquad (15)$$

$$O_2^{·-} \rightarrow\rightarrow\rightarrow H_2O_2 \qquad (16)$$

$$dAMP^{·+} + O_2^{·-} \rightarrow dAMP + O_2 \qquad (17)$$

$$dAMP^{·+} + O_2^{·-}/O_2 \rightarrow 8\text{-oxodAMP and/or } dAMP_{(ox)} \qquad (18)$$
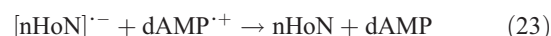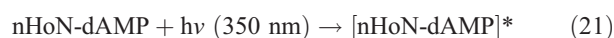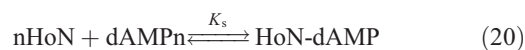
At pH 10.5. After the excitation of nHoN, even under alkaline conditions, the main active species in the first electronic excited state is [^{1}nHoH$^+$]* (reaction 19).[18]

$$nHoN + h\nu \ (350 \ nm) \rightarrow [^1nHoH^+]^* \qquad (19)$$
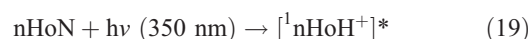
Thus, as in the case of pH 5, from [^{1}nHoH$^+$]* two competitive reactions can take place: (iv.3) the intrinsic photochemical pathway of *nor*harmane (reaction 10) and/or (iv.4) the photochemical pathways that yield the photooxidation of dAMP. However, the information provided herein is not enough to establish the mechanism involved in the latter reaction under alkaline pH conditions. On the one hand, fluorescence experiments indicate that [^{1}nHoH$^+$]* deactivation by dAMP takes place through a combination of both, dynamic and static interactions. On the other hand, kinetic analysis does not allow discarding either static or dynamic mechanism (numerical support, ESI†). Hence, at pH 10.5, the photosensitized reaction can take place (iv.4.1) either through a quite similar mechanism to that described above, where an nHoN–dAMP static complex is the species that absorbs the incident light leading to reactions 20 to 24:

(iv.4.1) (dAMP)$^{2-}$ photooxidation from the heterocomplex:. From now on (dAMP)$^{2-}$ will be written as dAMP.

$$nHoN + dAMPn \underset{}{\overset{K_s}{\rightleftharpoons}} HoN\text{-}dAMP \qquad (20)$$

$$nHoN\text{-}dAMP + h\nu \ (350 \ nm) \rightarrow [nHoN\text{-}dAMP]^* \qquad (21)$$

$$[nHoN\text{-}dAMP]^* \rightarrow [nHoN]^{·-} + dAMP^{·+} \qquad (22)$$

$$[nHoN]^{·-} + dAMP^{·+} \rightarrow nHoN + dAMP \qquad (23)$$

$$[nHoN]^{·-} + O_2 \rightarrow nHoN + O_2^{·-} \qquad (24)$$

The superoxide anion can then be deactivated through reactions 16–18, yielding H$_2$O$_2$, dAMP or 8-oxodAMP.

(iv.4.2) Through a dynamic mechanism where the neutral form of *nor*harmane (nHoN) absorbs the incident radiation leading to the formation of [^{1}nHoH$^+$]* (reaction 19) that diffuses and reacts with dAMP (charge transfer reaction) yielding

[nHoN]$^{\cdot-}$ and dAMP$^{\cdot+}$ radicals (reaction 25). Then, the latter radicals can follow reactions 14, 15, 17 and 18.

$$[^1\text{nHoH}^+]^* + \text{dAMP} + \text{OH}^- \rightarrow [\text{nHoN}]^{\cdot-} + \text{dAMP}^{\cdot+} + \text{H}_2\text{O} \quad (25)$$
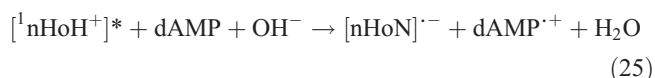
Conclusions

In this work we have proved that the interaction between *nor*harmane and dAMP, both in their electronic ground states, shows a strong pH-dependence that can be explained in terms of the chemical structure of both molecules. Then, the contribution of π-stacking between the alkaloid and the nucleobase (adenine) and coulombic interactions (due to the presence of net charge) would depend on the pH. Theoretical modeling suggests that the *nor*harmane molecule mainly interacts with the nucleobase adenosine by π-stacking but also the phosphate group plays a key role in the relative orientation of the two molecules.

Fluorescence studies reveal that under acidic conditions (at pH 2.5–5.4), where nHoH$^+$ is present, the singlet excited state of the acid form of *nor*harmane ([^{1}nHoH$^+$]*) is deactivated by dAMP *via* a purely static process. On the other hand, in alkaline media (pH 10.5), where the neutral form of *nor*harmane (nHoN) is predominant, the quenching involves a combination of dynamic and static processes, showing a relatively high efficiency of singlet excited state deactivation. In the whole pH range investigated, K_{SS} values indicate that association between *nor*harmane and dAMP takes place, but the formation of the corresponding complexes will be significant only at relatively high reactant concentrations.

In addition, we have demonstrated that, although extremely slow, the oxidation of dAMP photosensitized by *nor*harmane (under UV-A irradiation) takes place only in the presence of O$_2$. During this process O$_2$ is consumed and H$_2$O$_2$ is generated. To the best of our knowledge, this is the first time that evidence of photosensitized oxidation of dAMP by *nor*harmane is reported. The efficiency of the photosensitized reaction showed a pH-dependence and, at least under those pH conditions where the protonated form of *nor*harmane is present, a previous static complexation between the alkaloid and the nucleotide, both in their electronic ground states, is needed. The lower rate of dAMP consumption observed under alkaline solution can be explained, mainly, in terms of the photochemical and photophysical properties of *nor*harmane in aqueous solutions. ROS such as ^{1}O$_2$ does not participate in the photosensitization of dAMP by *nor*harmane.

The products of the studied process were analyzed by means of ESI-MS and UV-LDI-MS. After a quite long elapsed irradiation time, at least one main product, with a molecular weight of 347, was detected, which can be assigned to 8-oxo-7,8-dihydro-2′-deoxyadenosine 5′-monophosphate (8-oxodAMP). This fact suggests that the photosensitized oxidation takes place *via* a type I mechanism.

Finally, in connection with our previous finding related to the DNA damage photosensitized by βCs, results presented herein suggest that dAMP would not be the main target on the DNA photosensitization. This hypothesis is based on the fact that a π-stacked heterocomplex between the electronic ground state of *nor*harmane and dAMP is needed as a starting point for the dAMP photooxidation. Such a complex only can be formed when dAMP is present as a monomer because, as it was already demonstrated, the *nor*harmane moiety does not intercalate into the DNA double helix. In order to further investigate this hypothesis more experiments are in progress in our laboratory.

Notes and references

1 B. Hemmateenejad, A. Abbaspour, H. Maghami, R. Miri and M. R. Panjehshahin, *Anal. Chim. Acta*, 2006, **575**, 290–299.
2 H. P. Bais, S.-W. Park, F. R. Stermitz, K. M. Halligan and J. M. Vivanco, *Phytochemistry*, 2002, **61**, 539–543.
3 T.-S. Kam, K.-M. Sim, T. Koyano and K. Komiyama, *Phytochemistry*, 1999, **50**, 75–79.
4 P. S. Kearns, J. C. Cou and J. A. Rideout, *J. Nat. Prod.*, 1995, **58**, 1075–1076.
5 C. de Meester, *Mutat. Res., Rev.Genet. Toxicol.*, 1995, **339**, 139–153.
6 W. Pfau and K. Skog, *J. Chromatogr., B: Anal. Technol. Biomed. Life Sci.*, 2004, **802**, 115–126.
7 R. Spijkerman, R. van den Eijnden, D. van de Mheen, I. Bongers and D. Fekkes, *Eur. Neuropsychopharmacol.*, 2002, **12**, 61–71.
8 E. D. Cox and J. M. Cook, *Chem. Rev.*, 1995, **95**, 1797–1842.
9 K. Pari, C. S. Sundari, S. Chandani and D. Balasubramanian, *J. Biol. Chem.*, 2000, **275**, 2455–2462.
10 J. Torreilles, M. Guerin and A. Previero, *Biochimie*, 1985, **67**, 929.
11 U. Breyer-Pfaff, G. Wiatr, I. Stevens, H. Gaertner, G. Mundle and K. Mann, *Life Sci.*, 1996, **58**, 1425–1432.
12 T. Mori, A. Nakagawa, N. Kobayashi, M. W. Hashimoto, K. Wakabayashi, K. Shimoi and N. Kinae, *J. Radiat. Res.*, 1998, **39**, 21.
13 C. Chang, M. Castellazzi, T. Glover and J. Trosko, *Cancer Res.*, 1978, **38**, 4527.
14 K. Shimoi, H. Kawabata and I. Tomita, *Mutat. Res., Fundam. Mol. Mech. Mutagen.*, 1992, **268**, 287.
15 R. A. Larson, K. A. Marley, R. W. Tuveson and M. R. Berenbaum, *Photochem. Photobiol.*, 1988, **48**, 665–674.
16 J. B. Hudson, E. A. Graham and G. H. N. Towers, *Photochem. Photobiol.*, 1986, **43**, 21.
17 K. R. Downum, *New Phytol.*, 1992, **122**, 401–420.
18 M. M. Gonzalez, M. L. Salum, Y. Gholipour, F. M. Cabrerizo and R. Erra-Balsells, *Photochem. Photobiol. Sci.*, 2009, **8**, 1139–1149.
19 M. M. Gonzalez, J. Arnbjerg, M. P. Denofrio, R. Erra-Balsells, P. R. Ogilby and F. M. Cabrerizo, *J. Phys. Chem. A*, 2009, **113**, 6648–6656.
20 F. M. Cabrerizo, J. Arnbjerg, M. P. Denofrio, R. Erra-Balsells and P. R. Ogilby, *ChemPhysChem*, 2010, **11**, 796–798.
21 I. X. García-Zubiri, H. D. Burrows, J. S. Seixas de Melo, J. Pina, M. Monteserín and M. J. Tapia, *Photochem. Photobiol.*, 2007, **83**, 1455–1464.
22 H. Guan, X. Liu, W. Peng, R. Cao, Y. Ma, H. Chen and A. Xu, *Biochem. Biophys. Res. Commun.*, 2006, **342**, 894–901.
23 M. M. Gonzalez, M. Pellon-Maison, M. A. Ales-Gandolfo, M. R. Gonzalez-Baró, R. Erra-Balsells and F. M. Cabrerizo, *Org. Biomol. Chem.*, 2010, **8**, 2543–2552.

This journal is © The Royal Society of Chemistry 2012

Org. Biomol. Chem., 2012, **10**, 9359–9372 | 9371

24 M. M. Gonzalez, M. Vignoni, M. Pellon-Maison, M. A. Ales-Gandolfo, M. R. Gonzalez-Baró, R. Erra-Balsells, B. Epe and F. M. Cabrerizo, *Org. Biomol. Chem.*, 2012, **10**, 1807–1819.

25 All full aromatic βCs possess a *nor*harmane-like skeleton moiety, and the difference between them is the nature and position of the substituents. Therefore, the use of *nor*harmane as a model of βC is a reasonable starting point.

26 J. R. Lakowicz, *Principles of Fluorescence Spectroscopy*, Springer, New York, 2006, pp. 278–285.

27 G. Petroselli, M. L. Dántola, F. M. Cabrerizo, C. Lorente, A. M. Braun, E. Oliveros and A. H. Thomas, *J. Phys. Chem. A*, 2009, **113**, 1794–1799.

28 D. B. Davies, D. A. Veselkov, L. N. Djimant and A. N. Veselkov, *Eur. Biophys. J.*, 2001, **30**, 354–366.

29 M. P. Heyn, C. U. Nicola and G. Schwarz, *J. Phys. Chem.*, 1977, **81**, 1611–1617.

30 N. D'Amelio, L. Fontanive, F. Uggeri, F. Suggi-Liverani and L. Navarini, *Food Biophys.*, 2009, **4**, 321–330.

31 J. M. Ruso, D. Attwood, P. Taboada, V. Mosquera and F. Sarmiento, *Langmuir*, 2000, **16**, 1620–1625.

32 J. M. Ruso, P. Taboada, D. Attwood, V. Mosquera and F. Sarmiento, *Phys. Chem. Chem. Phys.*, 2000, **2**, 1261–1265.

33 J. Reuben, *J. Am. Chem. Soc.*, 1973, **95**, 3534–3540.

34 E. Gaggelli, N. D'Amelio, N. Gaggelli and G. Valensin, *Eur. J. Inorg. Chem.*, 2000, 1699–1706.

35 M. J. Vainio and M. S. Johnson, *J. Chem. Inf. Model.*, 2007, **47**, 2462–2474.

36 J. J. P. Stewart, MOPAC2009, *Stewart Computational Chemistry*, Colorado Springs, CO, USA, http://OpenMOPAC.net, 2008.

37 G. Petroselli, R. Erra-Balsells, F. M. Cabrerizo, C. Lorente, A. L. Capparelli, A. M. Braun, E. Oliveros and A. H. Thomas, *Org. Biomol. Chem.*, 2007, **5**, 2792–2799.

38 M. P. Denofrio, A. H. Thomas and C. Lorente, *J. Phys. Chem. A*, 2010, **114**, 10944–10950.

39 A. H. Thomas, R. Cabrerizo, M. Vignoni, R. Erra-Balsells, F. M. Cabrerizo and A. L. Capparelli, *Helv. Chim. Acta*, 2006, **89**, 1090–1104.

40 H. Nonami, K. Tanaka, Y. Fukuyama and R. Erra-Balsells, *Rapid Commun. Mass Spectrom.*, 1998, **12**, 285–296.

41 I. X. García-Zubiri, H. D. Burrows, J. S. Seixas de Melo, M. Monteserín, A. Arroyo and M. J. Tapia, *J. Fluoresc.*, 2008, **18**, 961–972.

42 Z. Miskolczy, M. Megyesi, L. Biczók and H. Görner, *Photochem. Photobiol. Sci.*, 2011, **10**, 592–600.

43 R. Tribolet and H. Sigel, *Biophys. Chem.*, 1987, **27**, 119–130.

44 Given the self-association equilibrium constants (K_{sa}) estimated in this work, under both pH conditions, at 1 mM of reactant concentration both (*nor*harmane and dAMP) are in their monomeric forms (>99.5%).

45 K. P. Ghiggino, P. F. Skilton and P. J. Thistlethwaite, *J. Photochem.*, 1985, **31**, 113–121.

46 Moreover, τ_F^0 value obtained here is in disagreement with τ_F^0 value previously reported by Ghiggino *et al.*[45] Our findings suggest that the quenching of *nor*harmane fluorescence by the OH⁻ ion described by the authors would be noticeable at pH > 10.5.

47 J. Řezáč, J. Fanfrlík, D. Salahub and P. Hobza, *J. Chem. Theory Comput.*, 2009, **5**, 1749–1760.

48 H. Sigel and R. Griesser, *Chem. Soc. Rev.*, 2005, **34**, 875–900.

49 T. Sengupta, S. D. Choudhury and S. Basu, *J. Am. Chem. Soc.*, 2004, **126**, 10589–10593.

50 G. Petroselli, M. L. Dántola, F. M. Cabrerizo, A. L. Capparelli, C. Lorente, E. Oliveros and A. H. Thomas, *J. Am. Chem. Soc.*, 2008, **130**, 3001–3011.

51 F. Wilkinson, H. P. Helman and A. B. Ross, *J. Phys. Chem. Ref. Data*, 1995, **24**, 663–677.

52 T. Douki and J. Cadet, *Int. J. Radiat. Biol.*, 1999, **75**, 571–581.

53 H. Nonami, S. Fukui and R. Erra-Balsells, *J. Mass Spectrom.*, 1997, **32**, 287–296.

54 S. Frelon, T. Douki, J.-L. Ravanat, J.-P. Pouget, C. Tornabene and J. Cadet, *Chem. Res. Toxicol.*, 2000, **13**, 1002–1010.

55 D. Angelov, A. Spassky, M. Berger and J. Cadet, *J. Am. Chem. Soc.*, 1997, **119**, 11373–11380.